International Journal of Mathematics and Computational Science
Vol. 2, No. 2, 2016, pp. 34-42
http://www.aiscience.org/journal/ijmcs
ISSN: 2381-7011 (Print); ISSN: 2381-702X (Online)

Effects of Chemical Reaction and Radiation on MHD Flow of a Viscous Fluid in a Vertical Channel with Non-uniform Concentration

K. Ramesh Babu[1], B. Venkateswarlu[2, *], P. V. Satya Narayana[3]

[1]Department of Mathematics, Sree Vidyanikethan Engineering College, Tirupati, A. P, India
[2]Department of Mathematics, MITS, Madanapalle, A. P, India
[3]Department of Mathematics, VIT, University, Vellore, T. N., India

Abstract

In this paper, we analyze the effects of chemical reaction and radiation on MHD mixed convective heat and mass transfer flow of a viscous fluid in a vertical channel with non-uniform concentration. The governing partial differential equations are transformed into a system of ordinary differential equations by non-dimensional procedure and are then solved by using regular perturbation method. The velocity, temperature and concentration profiles are analyzed graphically for different variations in the parameters. The physical interpretation to these expressions is examined through graphs and tables for the shear stress and rate of heat transfer coefficients at the vertical channel walls.

Keywords

Chemical Reaction, Thermal Radiation, MHD, Non-uniform Concentration

Received: August 1, 2015 / Accepted: August 12, 2015 / Published online: February 17, 2016

1. Introduction

Many engineering processes occur at high temperatures and consequently the radiation plays a significant role. Chandrasekhara and Nagaraju [1] examined the composite heat transfer in a variable porosity medium bounded by an infinite vertical flat plate in the presence of radiation. Yih [2] studied the radiation effects on natural convection over a cylinder embedded in porous media. Mohammadien and El-Amin [3] considered the thermal radiation effects on power law fluids over a horizontal plate embedded in a porous medium. Recently, Satya Narayana et al. [4] studied the effects of Hall current and radiation absorption on MHD micropolar fluid in a rotating system. Thermal radiation and heat source effects on a MHD nanofluid past a vertical plate in a rotating system with porous medium was investigated by [5].

The application of electromagnetic fields in controlling the heat transfer as in aerodynamic heating leads to the study of magneto hydrodynamics heat transfer. The MHD heat transfer has increased importance owing to advancement of space technology. So, it can be can divided into two sections, namely one contains problems in which the heating is an incidental by product of the electromagnetic fields as in the MHD generators and pumps etc. and the second contains of problems in which the primary use of electromagnetic fields is to control the heat transfer. With the fuel crisis deepening all over the world there is great concern to utilize the enormous power beneath the earth's crust in the geothermal region [6]. Liquid in the geothermal region is an electrically conducting liquid because of high temperature. Hence the study of interaction of the geomagnetic field with the fluid in the geothermal region is of great interest in the study of MHD convection flows through porous medium.

* Corresponding author
E-mail address: bvenkateswarlu.maths@gmail.com (B. Venkateswarlu)

The present trend in the field of chemical reaction analysis is to give a mathematical model for the system to predict the reactor enactment. Hence, a huge extent of research work has been reported in this direction. The study of heat and mass transfer with chemical reaction is of considerable importance in chemical and hydrometallurgical industries. The effect of chemical reaction can be codified as either heterogeneous or homogeneous processes. This depends on whether they occur at an interface or as a single phase volume reaction. Recently Venkateswarlu and Satya Narayana [7] investigated the chemical reaction and radiation absorption effects on the flow and heat transfer of a nanofluid in a rotating system. Several authors have studied the work on MHD flow through a porous medium in different geometries [8–10].

To the best of author's knowledge, the effects of chemical reaction and radiation on MHD mixed convective heat and mass transfer flow of a viscous fluid in a vertical channel with non-uniform concentration has unexplored. The coupled equations governing the flow, heat and mass transfer have been solved by using perturbation technique. The expression for the velocity, temperature and concentration profiles and as well as the rate of heat and mass transfer are derived and are analyzed for different values of the governing parameters.

2. Mathematical Formulation of the Problem

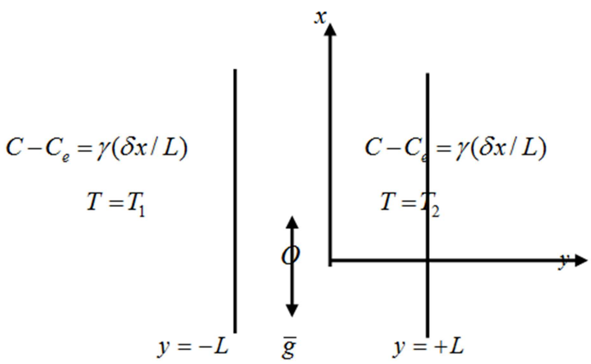

Figure 1. Configuration of the problem.

We consider the motion of viscous, incompressible fluid through a porous medium in a vertical channel bounded by flat walls. The thermal buoyancy in the flow field is created due to the non-uniform concentration on the walls $y=\pm L$ while both the walls are maintained at uniform temperatures. The Boussinesq approximation is used so that the density variation will be considered only in the buoyancy force. The viscous and Darcy dissipations are neglected in comparison to the heat conduction in the energy equation. Also the kinematic viscosity ν, the thermal conducting k are treated as constants. We choose a rectangular Cartesian system $O(x,y)$ with $x-$axis in the vertical direction and $y-$axis normal to the walls. The walls of the channel are at $y=\pm L$.

The equations governing the steady flow, heat and mass transfer are

$$\frac{\partial u}{\partial x}+\frac{\partial v}{\partial y}=0 \tag{1}$$

$$u\frac{\partial u}{\partial x}+v\frac{\partial u}{\partial y}=-\frac{1}{\rho_e}\frac{\partial p}{\partial x}+\frac{\mu}{\rho_e}\left\{\frac{\partial^2 u}{\partial x^2}+\frac{\partial^2 u}{\partial y^2}\right\} -\frac{\rho g}{\rho_e}-\left\{\frac{\sigma\mu_e^2 H_o^2}{\rho_e}\right\}u \tag{2}$$

$$u\frac{\partial v}{\partial x}+v\frac{\partial v}{\partial y}=-\frac{1}{\rho_e}\frac{\partial p}{\partial y}+\frac{\mu}{\rho_e}\left\{\frac{\partial^2 v}{\partial x^2}+\frac{\partial^2 v}{\partial y^2}\right\} \tag{3}$$

$$u\frac{\partial T}{\partial x}+v\frac{\partial T}{\partial y}=\frac{\lambda}{\rho_e C_p}\left\{\frac{\partial^2 T}{\partial x^2}+\frac{\partial^2 T}{\partial y^2}\right\} -\frac{Q_H}{\rho_e C_p}(T-T_e)-\frac{1}{\rho_e C_p}\frac{\partial q_r}{\partial y} \tag{4}$$

$$u\frac{\partial C}{\partial x}+v\frac{\partial C}{\partial y}=D\left\{\frac{\partial^2 C}{\partial x^2}+\frac{\partial^2 C}{\partial y^2}\right\}-k_r^*(C-C_e) \tag{5}$$

$$\rho-\rho_e=-\beta\rho_e(T-T_e)-\beta^*\rho_e(C-C_e) \tag{6}$$

We now assume Rosseland approximation (Brewester [11]), which leads to the radiative heat flux q_r is given by

$$q_r=-\frac{4\sigma^*}{3\beta_R}\frac{\partial T'^4}{\partial y} \tag{7}$$

If the temperature differences within the flow are sufficiently small such that T'^4 may be expressed as a linear function of the temperature, then the Taylor series for T'^4 about T_e, after neglecting higher order terms is given by

$$T'^4\approx 4T_e^3 T-3T_e^4 \tag{8}$$

In the equilibrium state

$$0=-\frac{\partial p_e}{\partial x}-\rho_e g \tag{9}$$

The flow is maintained by a constant volume flux for which a characteristic velocity is defined as

$$Q=\frac{1}{2L}\int_{-L}^{L} u\, dy \tag{10}$$

The boundary conditions for the velocity and temperature fields are

$$\begin{aligned} &u=0,\ v=0,\ \ T=T_1, C-C_e=\gamma(\delta x/L), on\ \ y=-L \\ &u=0,\ \ v=0,\ \ T=T_2, C-C_e=\gamma(\delta x/L), on\ \ y=L \end{aligned} \quad (11)$$

In view of the continuity equation we define the stream function ψ as

$$u=-\frac{\partial\psi}{\partial y}\, and\ \ v=\frac{\partial\psi}{\partial x} \quad (12)$$

Eliminating pressure p from equations (2)-(3) and using (7)-(8) the equations governing the flow in terms of ψ are

$$\begin{aligned} &\psi_x(\nabla^2\psi)_y-\psi_y(\nabla^2\psi)_x=\nu\nabla^4\psi-\beta g(T-T_0)_y \\ &-\beta^* g(C-C_0)_y-\frac{\sigma\mu_e H_o^2}{\rho_o}\frac{\partial^2\psi}{\partial y^2} \end{aligned} \quad (13)$$

$$\begin{aligned} &\frac{\partial\psi}{\partial y}\frac{\partial\theta}{\partial x}-\frac{\partial\psi}{\partial x}\frac{\partial\theta}{\partial y}=\frac{\lambda}{\rho_e C_p}\nabla^2\theta \\ &-\frac{Q_H}{\rho_e C_p}(T-T_o)+\frac{16\sigma^* T_e^3}{3\rho_e C_p\beta_R}\frac{\partial^2 T}{\partial y^2} \end{aligned} \quad (14)$$

$$\frac{\partial\psi}{\partial y}\frac{\partial C}{\partial x}-\frac{\partial\psi}{\partial x}\frac{\partial C}{\partial y}=D_1\nabla^2 C-k_r^*(C-C_o) \quad (15)$$

Introducing the non-dimensional variables in (13)-(15) as

$$x'=\frac{x}{L}, y'=\frac{y}{L}, \Psi'=\frac{\psi}{\nu}, \theta=\frac{T-T_2}{T_1-T_2}, C'=\frac{C-C_e}{\Delta C} \quad (16)$$

The governing equations in the non-dimensional form (after dropping the dashes) are

$$\frac{\partial(\psi,\nabla^2\psi)}{\partial(x,y)}=\frac{1}{\mathrm{Re}}\nabla^4\psi+\frac{Gr}{\mathrm{Re}^2}\left\{\theta_y+NC_y\right\}-\frac{M}{\mathrm{Re}}\frac{\partial^2\psi}{\partial y^2} \quad (17)$$

$$\begin{aligned} &\frac{\partial\psi}{\partial y}\frac{\partial\theta}{\partial x}-\frac{\partial\psi}{\partial x}\frac{\partial\theta}{\partial y}=\frac{1}{\mathrm{Re}\,P}\nabla^2\theta \\ &-\frac{Q}{\mathrm{Re}\,P}\theta+\frac{4}{3\,\mathrm{Re}\,PR}\frac{\partial^2\theta}{\partial y^2} \end{aligned} \quad (18)$$

$$\frac{\partial\psi}{\partial y}\frac{\partial C}{\partial x}-\frac{\partial\psi}{\partial x}\frac{\partial C}{\partial y}=\frac{1}{\mathrm{Re}\,Sc}\nabla^2 C-\frac{Kr}{\mathrm{Re}\,Sc}C \quad (19)$$

The corresponding boundary conditions are

$$\psi(+1)-\psi(-1)=1\ \frac{\partial\psi}{\partial x}=0, \frac{\partial\psi}{\partial y}=0\ at\ y=\pm1 \quad (20)$$

$$\begin{aligned} &C(x,y)=\gamma(\delta x), \theta=1 on\ \ y=-1 \\ &C(x,y)=\gamma(\delta\ x), \theta=0\ on\ \ y=+1 \end{aligned}$$

$$\frac{\partial\theta}{\partial y}=0, \frac{\partial C}{\partial y}=0 at\ \ y=0 \quad (21)$$

The value of ψ on the boundary assumes the constant volumetric flow in consistent with the hyphothesis (10). Also the wall concentration varies in the axial direction in accordance with the prescribed arbitrary function x.

3. Analysis of the Flow

The main aim of the analysis is to discuss the perturbations created over a combined free and forced convection flow due to non-uniform boundary temperature imposed on the boundaries.

Introduce the transformation such that $\bar{x}=\delta x, \frac{\partial}{\partial x}=\delta\frac{\partial}{\partial\bar{x}}$

Then $\frac{\partial}{\partial x}\approx O(\delta)\rightarrow\frac{\partial}{\partial\bar{x}}\approx O(1)$

For small values of $\delta<<1$, the flow develops slowly with axial gradient of order δ and hence we take $\frac{\partial}{\partial\bar{x}}\approx O(1)$ [See Refs. 12, 13]

Using the above transformation the equations (17-19) reduce to

$$\begin{aligned} &\frac{\partial(\psi,\nabla_1^2\psi)}{\partial(x,y)})=\frac{1}{\delta\mathrm{Re}}\nabla_1^4\psi \\ &+\frac{Gr}{\delta\mathrm{Re}^2}\left\{\theta_y+NC_y\right\}-\frac{M}{\delta\mathrm{Re}}\frac{\partial^2\psi}{\partial y^2} \end{aligned} \quad (22)$$

$$\frac{\partial\psi}{\partial y}\frac{\partial\theta}{\partial x}-\frac{\partial\psi}{\partial x}\frac{\partial\theta}{\partial y}=\frac{1}{\delta P\,\mathrm{Re}}\nabla_1^2\theta-\frac{Q}{\delta P\,\mathrm{Re}}\theta \quad (23)$$

$$\frac{\partial\psi}{\partial y}\frac{\partial C}{\partial x}-\frac{\partial\psi}{\partial x}\frac{\partial C}{\partial y}=\frac{1}{\delta Sc\,\mathrm{Re}}\nabla_1^2 C-\frac{Kr}{\delta Sc\,\mathrm{Re}}C \quad (24)$$

$$\nabla_1^2=\delta^2\frac{\partial^2}{\partial\bar{x}^2}+\frac{\partial^2}{\partial y^2} \quad (25)$$

We adopt the perturbation scheme and write

$$\begin{aligned} &\psi(x,y)=\psi_0(x,y)+\delta\psi_1(x,y)+\delta^2\psi\ _2(x,y)+ \\ &\theta(x,y)=\theta_0(x,y)+\delta\theta_1(x,y)+\delta^2\ \theta_2(x,y)+. \\ &C(x,y)=C_0(x,y)+\delta C_1(x,y)+\delta^2 C_2(x,y)+. \end{aligned} \quad (26)$$

On substituting (26) in (22)-(24) and separating the like powers of δ the equations and respective conditions to the zeroth order are

$$\psi_{0,yyyyy} - M_1^2\psi_{0,yy} = -\frac{Gr}{\text{Re}}\left\{\theta_{0,y} + NC_{0,y}\right\} \quad (27)$$

$$\theta_{0,yy} - Q\theta_0 = 0 \quad (28)$$

$$C_{0,yy} - Kr\,C_0 = 0 \quad (29)$$

The corresponding boundary conditions are

$$\psi_0(+1) - \psi_0(-1) = 1, \psi_{0,x} = 0, \psi_{0,y} = 0 at\ y = \pm 1 \quad (30)$$

$$\begin{aligned} &C_0 = \gamma(\bar{x}), \theta_0 = 1, C_0 = 1 \quad on \quad y = -1 \\ &C_0 = \gamma(\bar{x}), \theta_0 = 0, C_0 = 0 \quad on \quad y = 1 \end{aligned} \quad (31)$$

The first order equations are

$$\begin{aligned} &\psi_{1,yyyyy} - M_1^2\psi_{1,yy} = -\frac{Gr}{\text{Re}}\left\{\theta_{1,y} + NC_{1,y}\right\} \\ &+\text{Re}\left\{\psi_{0,y}\psi_{0,xyy} - \psi_{0,x}\psi_{0,yyy}\right\} \end{aligned} \quad (32)$$

$$\theta_{1,yy} - Q\theta_0 = P\,\text{Re}\left\{\psi_{0,x}\theta_{o,y} - \psi_{0,y}\theta_{ox}\right\} \quad (33)$$

$$C_{1,yy} - KrC_0 = Sc\,\text{Re}\left\{\psi_{0,x}C_{o,y} - \psi_{0,y}C_{ox}\right\} \quad (34)$$

The corresponding boundary conditions are

$$\begin{aligned} &\psi_1(+1) - \psi_1(-1) = 1 \\ &\psi_{1,x} = 0, \psi_{1,y} = 0, at\ y = \pm 1 \\ &\theta_1(\pm 1) = 0, C_1(\pm 1) = 0, at\ \ y = \pm 1 \end{aligned} \quad (35)$$

The second order equations are

$$\begin{aligned} &\psi_{2,yyyyy} - M_1^2\psi_{2,yy} = -\frac{Gr}{\text{Re}}\left\{\theta_{2y} + NC_{2,y}\right\} \\ &+\text{Re}\begin{Bmatrix} \psi_{0,yyt} + \psi_{0,x}\psi_{1,yyy} \\ +\psi_{1,x}\psi_{0,yyy} - \psi_{oy}\psi_{1,xyy} - \psi_{1,y}\psi_{0,xyy} \end{Bmatrix} \end{aligned} \quad (36)$$

$$\theta_{21,yy} - Q\theta_2 = P\,\text{Re}\begin{Bmatrix} \psi_{0,x}\theta_{1,y} - \psi_{0,y}\theta_{1x} \\ -\psi_{1,y}\theta_{o,x} + \psi_{1,x}\theta_{o,y} \end{Bmatrix} \quad (37)$$

$$C_{2,yy} - Kr\,C_2 = Sc\,\text{Re}\begin{Bmatrix} \psi_{0,x}C_{1,y} - \psi_{0,y}C_{1x} \\ -\psi_{1,y}C_{o,x} + \psi_{1,x}C_{o,y} \end{Bmatrix} \quad (38)$$

The corresponding boundary conditions are

$$\begin{aligned} &\psi_2(+1) - \psi_2(-1) = 1 \\ &\psi_{2,x} = 0, \psi_{2,y} = 0, at\ y = \pm 1 \\ &\theta_2(\pm 1) = 0, C_2(\pm 1) = 0\ at\ \ y = \pm 1 \end{aligned} \quad (39)$$

Solving the equations (27)-(38) subject to the relevant boundary conditions, we obtain the required velocity, temperature and concentration for different values of the parameters entering in to the problem as

$$\varphi_0 = \gamma(x)\frac{Ch(\beta_1 y)}{Ch(\beta_1)}$$

$$\begin{aligned} \theta_0 &= 0.5\left\{\frac{Ch(\beta_2 y)}{Ch(\beta_2)} - \frac{Sh(\beta_2 y)}{Sh(\beta_2)}\right\} \\ &+a_3\left\{Ch(\beta_1 y) - Ch(\beta_1)C\frac{Ch(\beta_2 y)}{Ch(\beta_2)}\right\} \end{aligned}$$

$$\psi_o = a_{12}Ch(M_1 y) + a_{13}Sh(M_1 y) + a_{14}y + a_{15} + f_1(y)$$

$$f_1(y) = -a_9 Sh(\beta_2 y) - a_{10}Ch(\beta_2 y) - a_{11}Sh(\beta_1 y)$$

$$\begin{aligned} \phi_1 &= a_{32}Ch(\beta_3 y) + a_{33}Ch(\beta_4 y) \\ &+(a_{34} + a_{49})Ch(\beta_5 y) + a_{35}Ch(\beta_6 y) \\ &+a_{36}Sh(\beta_3 y) + (a_{37} + a_{48})Sh(\beta_4 y) \\ &+a_{38}Sh(\beta_5 y) + a_{39}Sh(\beta_6 y) \\ &+a_{40}Ch(2\beta_1 y) + a_{41}Sh(2\beta_1 y) + a_{42}y^2 \\ &+a_{45}(y^2 - 1)Ch(\beta_1 y) + a_{46}ySh(\beta_1 y) \\ &-\begin{Bmatrix} a_{32}Ch(\beta_3) + a_{33}Ch(\beta_4) \\ +(a_{34} + a_{49})Ch(\beta_5) \\ +a_{35}Ch(\beta_6) + a_{40}Ch(2\beta_1) \\ +a_{42} + a_{46}Sh(\beta_1) \end{Bmatrix}\frac{Ch(\beta_1 y)}{Ch(\beta_1)} \\ &-\begin{Bmatrix} a_{36}Sh(\beta_3) + (a_{37} + a_{48})Sh(\beta_4) \\ +a_{38}Sh(\beta_5) + a_{39}Sh(\beta_6) \\ +a_{41}Sh(2\beta_1) \end{Bmatrix}\frac{Sh(\beta_1 y)}{Sh(\beta_1)} + a_{42}y^2 \\ &+a_{45}(y^2 - 1)Ch(\beta_1 y) \end{aligned}$$

$$\theta_1 = a_{76}Ch(\beta_2 y) + a_{77}Sh(\beta_2 y) + f_2(y)$$

$$\begin{aligned} f_2(y) &= a_{49}Ch(\beta_1 y) + a_{50}Sh(\beta_1 y) \\ &+a_{51}ySh(\beta_1 y) + a_{52}yCh(\beta_1 y) \\ &+a_{53}ySh(\beta_2 y) + a_{54}yCh(\beta_2 y) \\ &+a_{55}y^2Ch(\beta_2 y) + a_{56}Ch(\beta_3 y) \\ &+a_{57}Ch(\beta_4 y) + a_{58}Ch(\beta_5 y) \\ &+a_{59}Ch(\beta_6 y) + a_{60}Ch(\beta_7 y) \\ &+a_{61}Ch(\beta_8 y) + a_{62}Sh(\beta_3 y) \\ &+a_{63}Sh(\beta_4 y) + a_{64}Sh(\beta_5 y) \\ &+a_{65}Sh(\beta_6 y) + a_{66}Sh(\beta_7 y) \\ &+a_{67}Sh(\beta_8 y) + a_{68}Ch(2\beta_2 y) \\ &+a_{69}Sh(2\beta_2 y) + a_{70} + a_{71}Ch(2\beta_1 y) \\ &+a_{72}y + a_{73}Sh(2\beta_1 y) \\ &+a_{74}y^2 + a_{75}y^2Ch(\beta_1 y) \end{aligned}$$

$$\psi_1 = b_{63}Ch(M_1 y) + b_{64}Sh(M_1 y) + f_4(y)$$

$$\begin{aligned}
f_4(y) &= (b_{29}+b_{49}+y(b_{51}+b_{34})+y^2 b_{52})Sh(\beta_2 y) \\
&+(b_{30}+b_{35}+yb_{48}+y^2 b_{50})Ch(\beta_2 y)+(b_{31}+y^2 b_{55})Sh(\beta_1 y) \\
&+(b_{32}+yb_{33})Ch(\beta_1 y)+b_{36}Ch(\beta_3 y) \\
&+b_{37}Ch(\beta_4 y)+b_{38}Ch(\beta_5 y) \\
&+b_{39}Ch(\beta_6 y)+b_{40}Ch(\beta_7 y) \\
&+b_{41}Ch(\beta_8 y)+b_{42}Sh(\beta_3 y)+b_{43}Ch(\beta_4 y)+b_{44}Ch(\beta_5 y) \\
&+b_{45}Ch(\beta_6 y)+b_{46}Ch(\beta_7 y)+b_{47}Ch(\beta_8 y) \\
&+b_{53}y^2+b_{54}y^3+b_{56}y^2 Sh(M_1 y)+b_{57}yCh(M_1 y) \\
&+b_{58}Sh(2M_1 y)+b_{59}Sh(2\beta_2 y)+b_{60}Sh(2\beta_1 y) \\
&+b_{61}Ch(2M_1 y)+b_{62}Ch(2\beta_2 y)
\end{aligned}$$

The local rate of heat transfer coefficient (Nusselt number Nu) on the walls has been calculated using the formula

$$Nu = \frac{1}{\theta_m - \theta_w}\left(\frac{\partial \theta}{\partial y}\right)_{y=\pm 1}$$

where $\theta_m = 0.5\int_{-1}^{1} \theta \, dy$

and the corresponding expressions are $Nu_{y=+1} = \frac{e_1 + \delta e_5}{\theta_m - 1}$

$$Nu_{y=-1} = \frac{e_2 + \delta e_6}{\theta_m}$$

where $\theta_m = e_9 + \delta e_{12}$

The local rate of mass transfer coefficient (Sherwood Number Sh) on the walls has been calculated using the formula

$$Sh = \frac{1}{C_m - C_w}\left(\frac{\partial C}{\partial y}\right)_{y=\pm 1}$$

where $C_m = 0.5\int_{-1}^{1} C \, dy$

and the corresponding expressions are

$$Sh_{y=+1} = \frac{e_3 + \delta e_7}{C_m - \gamma(x)}$$

$$Sh_{y=-1} = \frac{e_4 + \delta e_8}{C_m - \gamma(x)}$$

where $M_1 + \beta_1 = \beta_3, M_1 - \beta_1 = \beta_4, \beta_1 + \beta_2 = \beta_5, \beta_1 - \beta_2 = \beta_6$

$M_1 + \beta_2 = \beta_7, M_1 - \beta_2 = \beta_8$, $a_1 = \frac{\gamma(x)}{Ch\beta_2}$ $a_3 = \frac{s_c s_0}{N}\left(\frac{\gamma \beta_2^2}{Ch\beta_2}\right)$

The other constants are not given here to save space.

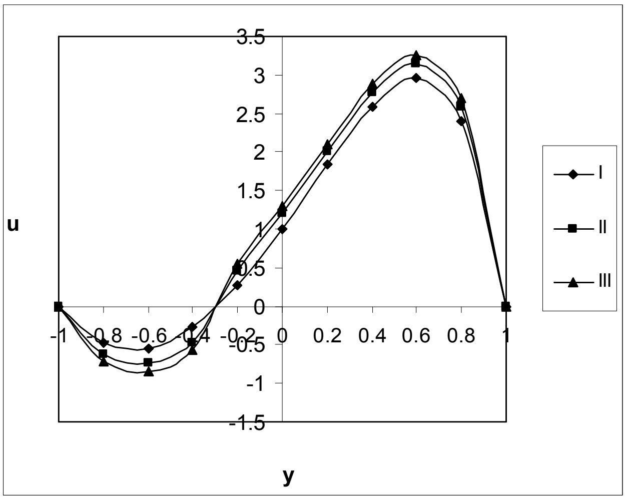

Figure 2(a). Axial Velocity for various values of *Kr*.

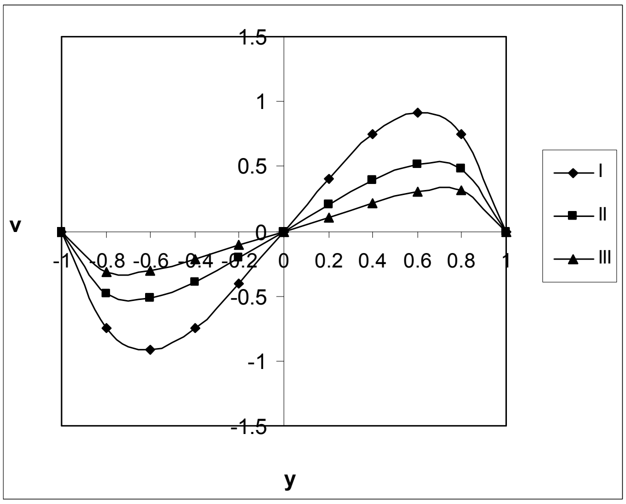

Figure 2(b). Secondary Velocity for various values of *Kr*.

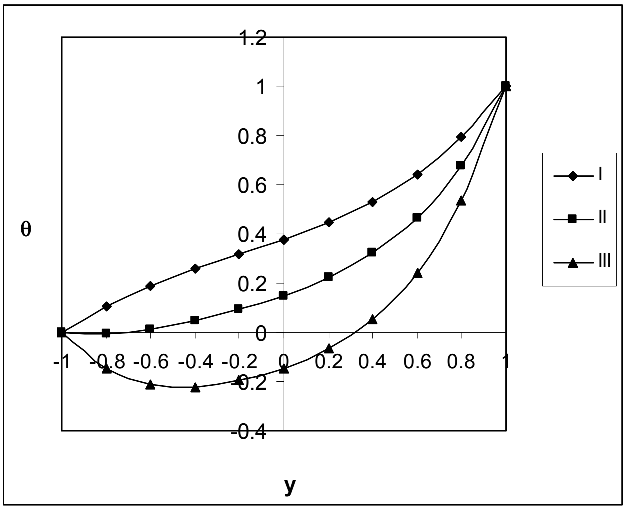

Figure 2(c). Temperature for various values of *Kr*.

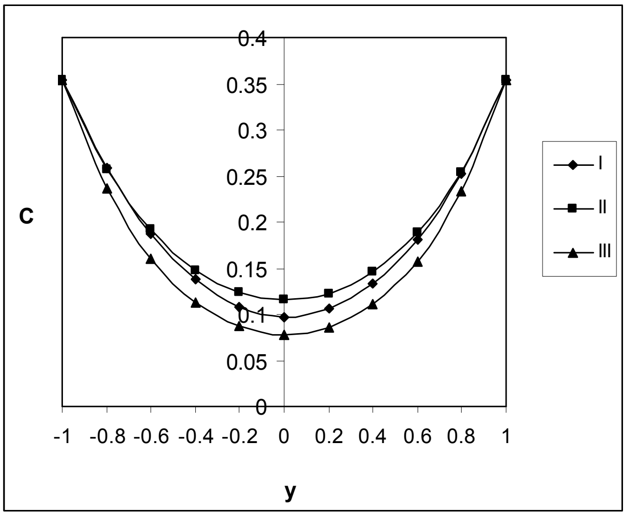

Figure 2(d). Concentration for various values of *Kr*.

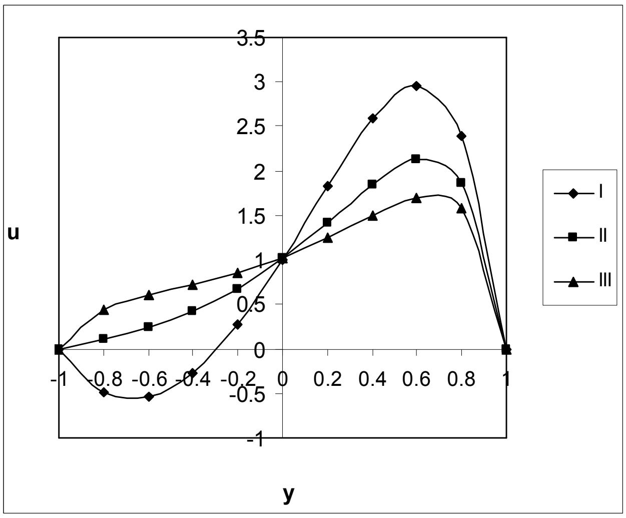

Figure 3(a). Axial Velocity for various values of *M*.

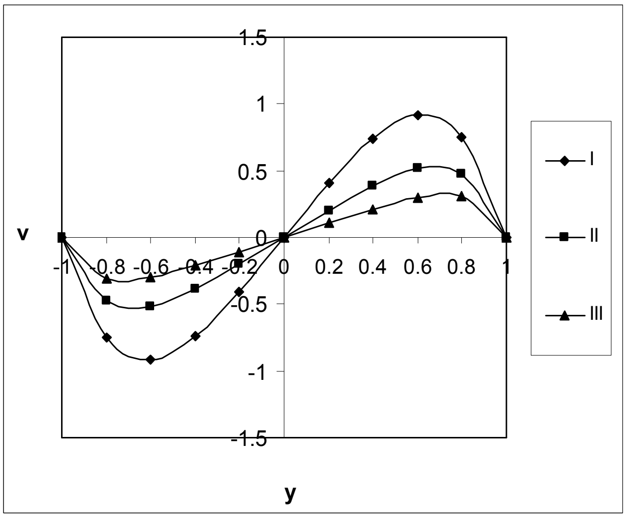

Figure 3(b). Secondary Velocity for various values of *M*.

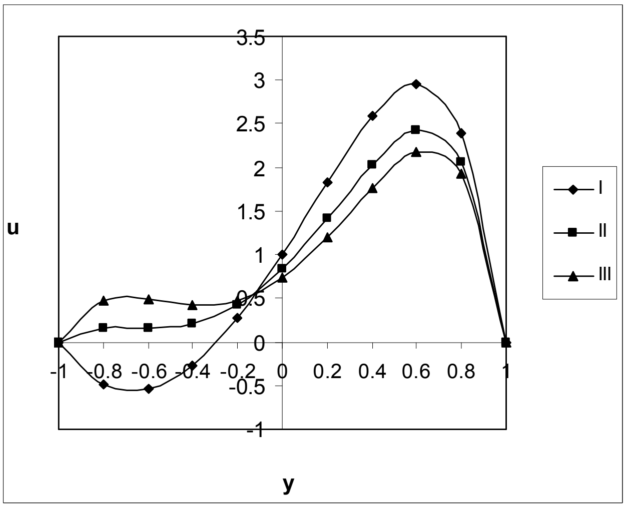

Figure 4(a). Axial Velocity for various values of *Q*.

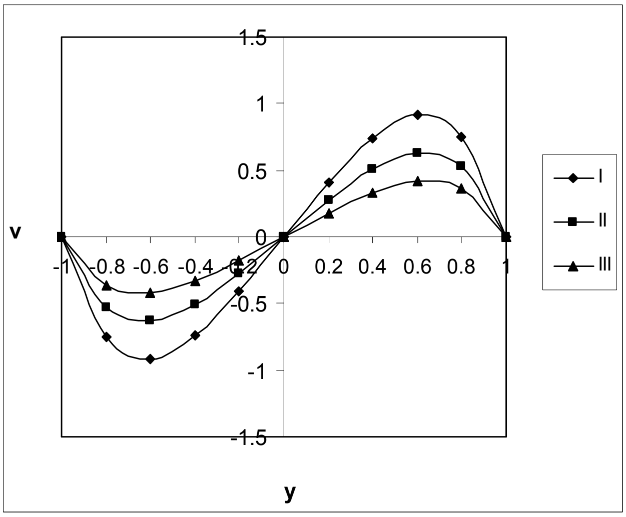

Figure 4(b). Secondary Velocity for various values of *Q*.

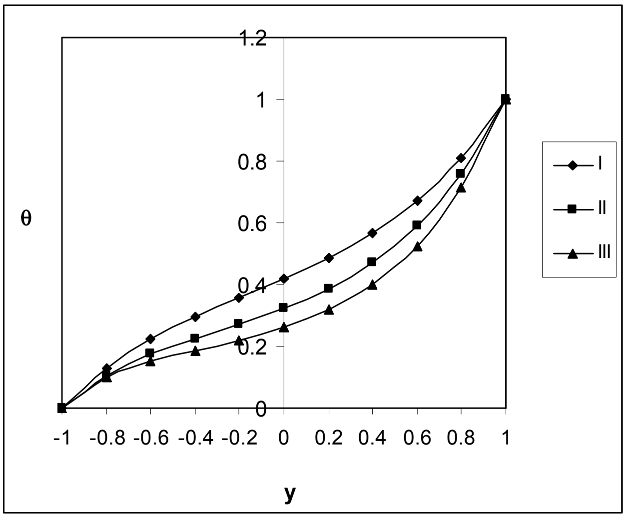

Figure 4(c). Temperature for various values of *Q*.

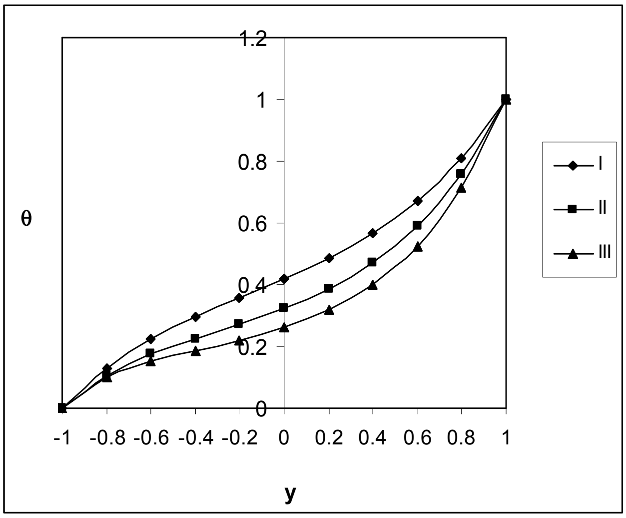

Figure 4(d). Concentration for various values of *Q*.

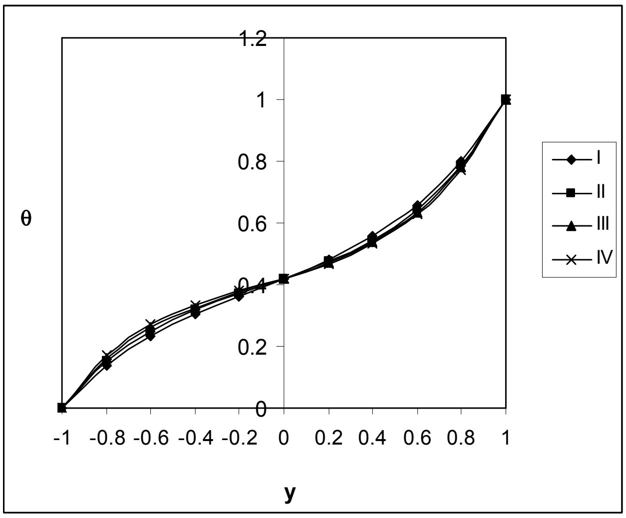

Figure 5(c). Temperature for various values of *R*.

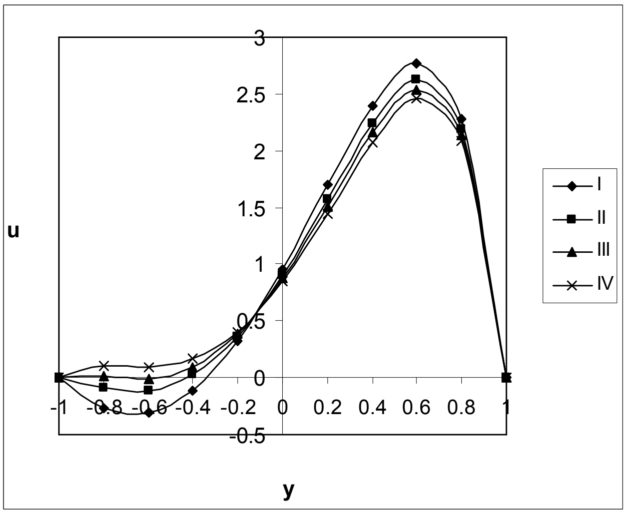

Figure 5(a). Axial Velocity for various values of *R*.

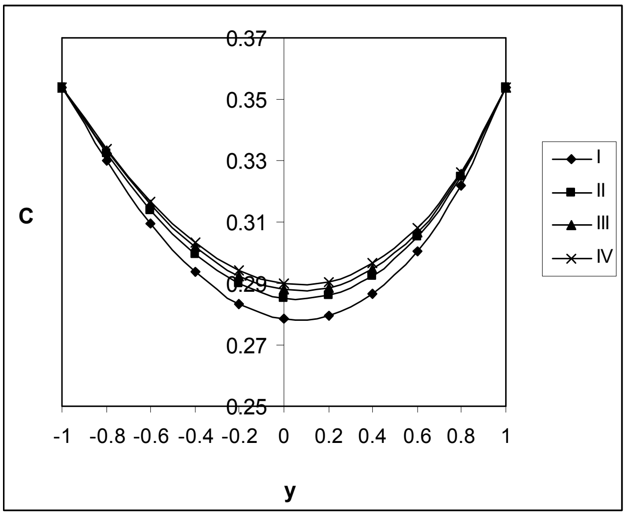

Figure 5(d). Concentration for various values of *R*.

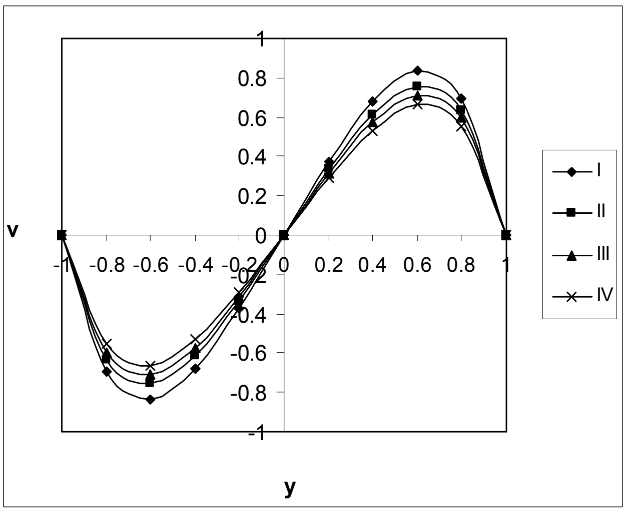

Figure 5(b). Secondary Velocity for various values of *R*.

4. Results and Discussion

In this analysis, we investigate the effects of chemical reaction and radiation on MHD mixed convective heat and mass transfer flow of a viscous electrically conducting fluid in a vertical channel with non-uniform concentration and constant wall temperatures. The wall concentration $\gamma(x)$ is taken as $\gamma(x) = \alpha \sin x$. The axial velocity (u) is shown in Figs 2-5 for different values of *Gr, Kr, M, N, R, Q, Sc*, α and *x*.

The variation of axial velocity, secondary velocity, temperature and concentration profiles are shown in Figs 2(a)-2(d) for different values of chemical reaction parameter *Kr*. It is clear from Figs 2(a) and 2(b) that both the axial and secondary velocities are depreciates in the degeneration reaction and enhances in the generating reaction. Further, from Figs 2(c) and 2(d) show that the variation of both the temperature and concentration profiles are reduces with increase in smaller and higher values of the chemical reaction parameter *Kr* and enhances with intermediate values of *Kr*.

The effects of magnetic field parameter *M* on the axial velocity, secondary velocity, temperature and concentration distributions are presented in graphs 3(a)-3(d). It is observed from Figs 3(a) and 3(b) that both the axial and secondary velocities with magnetic field parameter *M* shows the reversal flow which appears in the left half at M=2 disappears for higher $M \geq 4$. Thus, the magnitude of axial and secondary velocities are depreciates with higher Lorentz force in the region. Further, from Figs 3(c) and 3(d) shows that the temperature depreciates with magnetic field parameter *M* and that higher the Lorentz force higher the concentration.

The effects of heat source parameter *Q* on the axial velocity, secondary velocity, temperature and concentration profiles are shown in Figs 4(a)-4(d). The variation of both the axial and secondary velocities (u, v) with heat source parameter *Q* shows that the reversal which appears in the left half for *Q*=2 disappears for higher $\alpha \geq 4$. Thus the presence of heat generating sources reduces both the axial and secondary velocities in the entire flow region. Further, an increase in the heat source parameter *Q* reduces the temperature and whereas the results in an enhancement in concentration profiles. Thus the presence of the heat sources in the flow region leads to depreciation in the temperature and then concentration enhances.

The axial velocity, secondary velocity, temperature and concentration profiles are presented in Figs 5(a)-5(d) respectively, for different values of thermal radiation parameter R. With reference to thermal radiation parameter *R*, we find figure 5(a) that the reversal flow which appears in the vicinity of the left boundary for $R \leq 5$ disappears for higher $R \geq 10$. It is clear from Figs 5(b) that an increase in the thermal radiation parameter *R* reduces |v| in the flow region. Thus higher the radiative heat flux lesser the magnitude of the secondary velocity v. Further, an increase in the thermal radiation parameter *R* leads to a depreciation in the temperature and enhancement in the concentration profiles are clearly shows in Figs 5(c) and 5(d).

Table 1. Nusselt Number *Nu* at y=+1.

Gr	I	II	III	IV	V	VI
10^3	-2.6338	-2.0310	-1.5272	-3.4324	-3.8186	-2.0310
$3x10^3$	-1.7185	-1.3052	-1.0442	-2.4906	-3.1509	-1.3052
-10^3	-27.4207	4.1014	0.7048	-5.7528	-4.8821	4.1014
$-3x10^3$	1.4835	0.1115	-0.3557	-20.7427	-6.8414	0.1115
Kr	1.5	2.5	3.5	0.5	0.5	0.5
M	2.5	2.5	2.5	4.5	6.5	2.5
N	1	1	1	1	1	2
Q	2	2	2	2	4	6
R	35	70	140	35	35	35
Re	35	70	140	35	35	35
Sc	1.3	1.3	1.3	1.3	0.24	0.6
α	0.1	0.3	0.7	0.9	0.5	0.5
x	π/4	π/4	π/4	π/4	π/4	π/2

Table 2. Nusselt Number *Nu* at y=-1.

Gr	I	II	III	IV	V	VI
10^3	1.26413	3.39101	-17.46995	0.49012	0.40935	3.39101
$3x10^3$	14.16587	-5.06143	-2.83825	0.85683	0.53299	-5.06143
-10^3	-0.14866	-0.46918	-0.85353	0.24265	0.30593	-0.46918
$-3x10^3$	-0.69096	-1.07591	-1.39853	0.06441	0.21815	-1.07591
Kr	1.5	2.5	3.5	0.5	0.5	0.5
M	2.5	2.5	2.5	4.5	6.5	2.5
N	1	1	1	1	1	2
Q	2	2	2	2	4	6
R	35	70	140	35	35	35
Re	35	70	140	35	35	35
Sc	1.3	1.3	1.3	1.3	0.24	0.6
α	0.1	0.3	0.7	0.9	0.5	0.5
x	π/4	π/4	π/4	π/4	π/4	π/2

The average Nusselt number *Nu* at the boundary y=±1 is shown in Tables 1-2 for different values of *Gr*. An increase in the chemical reaction parameter *Kr* leads to an enhancement in |Nu| at both the walls. The variation of *Nu* with Hartman number *M* shows that higher the Lorentz force larger |Nu| at y=+1 and smaller at y=-1. When the molecular buoyancy force dominates over the thermal buoyancy force the rate of heat transfer reduces at y =+1 and enhances at y= -1 when the buoyancy forces act in the same direction and for the forces acting in opposite directions, |Nu| experiences an enhancement at both the walls. The variation of *Nu* with radiation parameter *N* shows that higher the radiative heat flux larger |Nu| at y= ±1 for *Gr*>0 and smaller at y=+1 and larger at y=-1 for *Gr*<0. The variation of Nu with heat source parameter *Q* shows that |Nu| enhances with increase in *Q*>0 at y = ±1 while for *Q*<0, it reduces at y = +1 and enhances at y = -1.

References

[1] B. G. Chandrasekhara, P. Nagaraju, Composite heat transfer in the case of a steady laminar flow of a gray fluid with small optical density past a horizontal plate embedded in a porous medium, Warm Stoffubentras, 23(6), (1998), 243–352.

[2] K. A. Yih, Radiation effects on natural convection over a vertical cylinder embedded in a porous media, International Journal of Communication in Heat Mass Transfer, 26(2), (1999), 259–267.

[3] A. A. Mohammadien, M.F. El. Amin, Thermal radiation effects on power-law fluids over a horizontal plate embedded in a porous medium, International Journal of com heat Mass, l27 (2), (2000), 1025–1035.

[4] P. V. Satya Narayana, B. Venkateswarlu, S. Venkataramana, Effects of Hall current and radiation absorption on MHD micropolar fluid in a rotating system, Ain Shams Engineering Journal, 4(4), (2013), 843–854.

[5] P. V. Satya Narayana, B. Venkateswarlu, S. Venkataramana, Thermal radiation and heat source effects on a MHD nanofluid past a vertical plate in a rotating system with porous medium, Journal of Heat Transfer Asian Research, 44(1), (2015).

[6] W. Somertone, J. M. McDonough, I. Cotton, Natural convection in volumetrically heated porous layer, Journal of Heat transfer, 1, (1984), 106–241.

[7] B. Venkateswarlu, P.V. Satya Narayana, Chemical reaction and radiation absorption effects on the flow and heat transfer of a nanofluid in a rotating system, Applied Nanoscience 5, (2015), 351–360.

[8] P. V. Satya Narayana, B. Venkateswarlu, MHD visco-elastic fluid flow over a continuously moving vertical surface with chemical reaction, Walailak Journal of Science and Technology, 12, (2015).

[9] K. Ramesh Babu, B. Venkateswarlu, P.V. Satya Narayana, Effects of chemical reaction and radiation absorption on mixed convective flow in a circular annulus at constant heat and mass flux. Advances in Applied Science Research, 5(5), (2014), 122–138.

[10] P. V. Satya Narayana, B. Venkateswarlu, S. Venkataramana, Chemical reaction and Radiation absorption effects on MHD micropolar fluid past a vertical porous plate in a rotating system, Journal of Energy Heat and Mass Transfer, 35, (2013), 197–214.

[11] M. Q. Brewester, Thermal radiation transfer and properties, John Wiley and sons. Inc. New York, (1992).

[12] D. R. V. Prasada Rao, D. V. Krishna, Lokenath Debnath, Combined effect of free and forced convection on MHD flow in a rotating porous channel, International Journal of Math. & Math. Science, 5, (1982), 165–182.

[13] D. R. V. Prasada Rao, D. V. Krishna, Lokenath Debnath, Free convection in hydromagnetic flows in a vertical wavy channel, International Journal of Engineering Science, 21(9), (1983), 1025–1039.